

# Topological band gap in intercalated epitaxial graphene

Minsung Kim,<sup>1</sup> Cai-Zhuang Wang,<sup>1,2</sup> Michael C. Tringides,<sup>1,2</sup> Myron Hupalo,<sup>1,2</sup> and Kai-Ming Ho<sup>1,2</sup>

<sup>1</sup>*Ames Laboratory – U.S. Department of Energy,  
Iowa State University, Ames, Iowa 50011, USA*

<sup>2</sup>*Department of Physics and Astronomy,  
Iowa State University, Ames, Iowa 50011, USA*

(Dated: January 14, 2022)

## Abstract

Functional manipulation of graphene is an important topic in view of both fundamental researches and practical applications. In this study, we show that intercalation of 5d transition metals in epitaxial graphene on SiC is a promising approach to realize topologically nontrivial phases with a finite band gap in graphene. Using first-principles calculations based on density functional theory, we show that the Re- and Ta-intercalated graphene become two-dimensional topological insulators which exhibit linear Dirac cones and quadratic bands with topological band gaps, respectively. The appearance of the topological states is attributed to the strong spin-orbit coupling strength of the intercalants. We find that topological edge states exist within the finite bulk band gap in accordance with the bulk-boundary correspondence. We also discuss the spin splitting of the band structure due to the inversion symmetry breaking and the spin-orbit coupling. Our results demonstrate that intercalation of graphene is an effective and viable method to manipulate the band gap and the topological character of graphene. Such intercalated graphene systems are potentially useful for spintronics and quantum computing applications.

Low-dimensional material has been a primary theoretical and experimental interest in condensed matter physics, chemistry, and materials science since the first synthesis of graphene [1–3]. One of the most important aspects of this two-dimensional (2D) atomically-thin carbon layer is that it allows functional manipulation of electronic properties via physical or chemical interactions with the substances adjacent to it, e.g., using molecular adsorption, heterostructure, or intercalation. In particular, intercalation was shown to be a useful method to affect the quasi-particle excitation, superconductivity, adsorption energy of adatoms, etc. [4–9]. It was demonstrated that the intercalation controls the coupling between a substrate and a graphene layer, and can further change the band character of Dirac cones in graphene [4–6, 10–12].

Among many intriguing electronic properties of graphene, the quantum spin Hall (QSH) phase (i.e., the 2D topological insulator phase) attracted noticeable interest [13, 14]. Theoretically, the carbon honeycomb lattice is expected to show the QSH effect characterized by the nontrivial  $\mathbb{Z}_2$  topological number [15, 16]. However, the essential ingredient of topological phases is spin-orbit coupling (SOC) which is small in graphene [17]. The SOC-induced band gap of pristine graphene is estimated to be  $10^{-3}$  meV which is negligible in practice. Since the gapless band structure sets fundamental limitation in the application of graphene in comparison with other conventional semiconductors with finite gaps, the enhancement of the SOC strength is important for the utility of graphene as well as the realization of the novel topological phase.

In this study, we consider the intercalation of  $5d$  transition metal atoms that has significant SOC strength to enhance the topological band gap of graphene. Given that the intercalation can give rise to qualitatively different Dirac cones with significant contributions from intercalant orbital states [12], it is plausible to expect that the intercalation of such heavy elements would enhance the SOC effects in the Dirac cones. After a systematic calculation of the electronic band structures of the epitaxial graphene on SiC substrate with  $5d$  transition metal (from Hf to Ir in the periodic table) intercalation, we find that 2D topological insulator phases are indeed achieved for suitable choices of the intercalants. Specifically, we show that the Re-intercalated epitaxial graphene has topological Dirac cones at the Fermi energy. We find that the SOC induces a finite topological band gap with nontrivial  $\mathbb{Z}_2$  band topology of the occupied bands. Correspondingly, the spin-polarized topological edge states appear due to the nontrivial 2D bulk band topology as dictated by bulk-boundary corre-

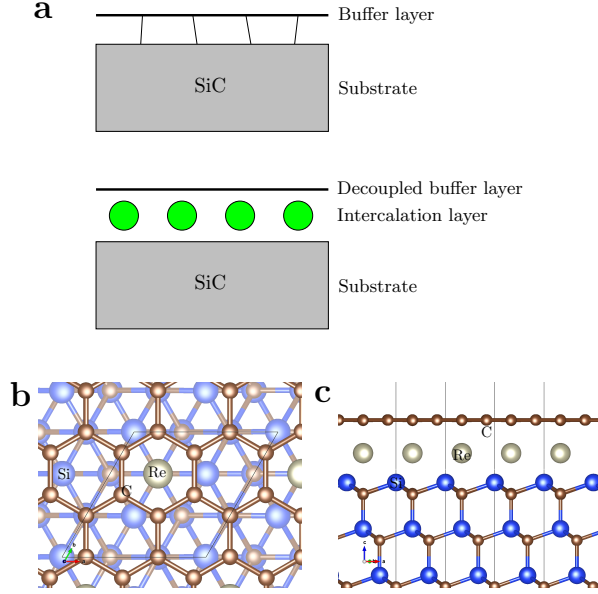


FIG. 1. Atomic structure of Re-intercalated epitaxial graphene on SiC. (a) Schematic illustration. (b) Top and (c) side view of the atomic structure.

spondence. In the case of the Ta intercalation, the electronic band structure near the Fermi level shows quadratic band dispersion (as opposed to linear one in the Re intercalation) with a topological band gap. We also show that the spin splitting of the band structures near the band edges is originated from the broken inversion symmetry and the SOC.

The electronic band structures were calculated using a first-principles method based on density functional theory (DFT) as implemented in VASP package [18, 19]. We employed the projector augmented-wave (PAW) method [20, 21] and used a plane-wave basis set with 400 eV energy cutoff.  $\Gamma$ -centered  $12 \times 12 \times 1$   $k$ -point meshes were exploited. For the atomic structure, we considered  $\sqrt{3} \times \sqrt{3}$  cell of the Si-terminated SiC substrate (consisting of 4 SiC layers) which may accommodate  $2 \times 2$  graphene layer on top of it. An experimental lattice constant of SiC (type 6H) was used [22], and the internal atomic coordinates were relaxed until the force acting on each atom became less than  $0.02 \text{ eV}/\text{\AA}$  while the 2 lowest SiC layers were fixed. The Re and Ta metal atoms were intercalated between the outermost Si layer and the graphene layer (i.e., decoupled buffer layer). A sufficiently thick vacuum region ( $\gtrsim 20 \text{ \AA}$ ) was employed to prevent the unwanted interaction between periodic images. Wannier functions were obtained using Wannier90 [23] and edge state dispersions were calculated using WannierTools [24].

The intercalation induces decoupling of the graphene layer from the SiC substrate. In the epitaxial graphene on SiC substrate, the first carbon layer (called buffer layer or 0th layer) makes strong chemical bonds with the outermost Si atoms. Due to the strong hybridization, this buffer layer does not possess Dirac cones unlike pristine graphene [5, 6]. The intercalation can decouple the buffer layer from the substrate reviving the Dirac cones of the graphene (i.e., decoupled buffer layer) [4–6, 10, 11, 25, 26]. For instance, the intercalation of Au was experimentally shown to control the coupling between the buffer layer and the substrate as demonstrated by the appearance of Dirac cones upon intercalation using angle-resolved photoemission spectroscopy (ARPES) [5]. In our present study the intercalation of the Re or Ta layer (Fig. 1) is also expected to decouple the buffer layer from the SiC substrate and change the effective SOC strength in the graphene layer.

We find that the electronic band structure of the Re-intercalated epitaxial graphene has Dirac cones with a sizable SOC-induced band gap. Figure 2 shows the electronic band structures obtained from our DFT calculations. Without the SOC, the band structure has a Dirac cone at the  $K$  point of the Brillouin zone (BZ) as in pristine graphene. However, upon including the SOC, there appears a finite band gap at the Dirac point ( $\approx 107$  meV) in contrast to pristine graphene. To understand the origin of the SOC-induced gap, we calculate the orbital contributions of the Dirac cone states (Fig. 2c). In pristine graphene, the Dirac cone at the  $K$  point consists of C  $p_z$  orbital. In contrast, in the epitaxial graphene with the Re intercalation, we find that there are significant contributions from Re  $d$  states as well as the graphene C  $p_z$ . Thus, we have the sizable SOC-induced gap opening in the Re-intercalated epitaxial graphene whereas the effect of SOC on the band gap is negligible in pristine graphene.

To examine the topological feature of the intercalated epitaxial graphene, we calculate the  $\mathbb{Z}_2$  topological invariant that characterizes the band topology of a 2D gapped system [27]. The topological number is defined as

$$\nu = \frac{1}{2\pi} \left\{ \oint_{\partial B_{1/2}} A - \int_{B_{1/2}} F \right\} \text{ mod } 2, \quad (1)$$

where  $A$ ,  $F$ , and  $B_{1/2}$  represent the Berry connection, the Berry curvature, and the half of the BZ, respectively. In practice, this integral formula is computed on a discretized  $k$ -mesh in DFT calculations and the corresponding topological number becomes a sum of an integer field  $n(\vec{k})$  as  $\nu = \sum_{\vec{k}_i \in B_{1/2}} n(\vec{k}_i) \text{ mod } 2$  [28, 29]. Whereas the topological Chern number

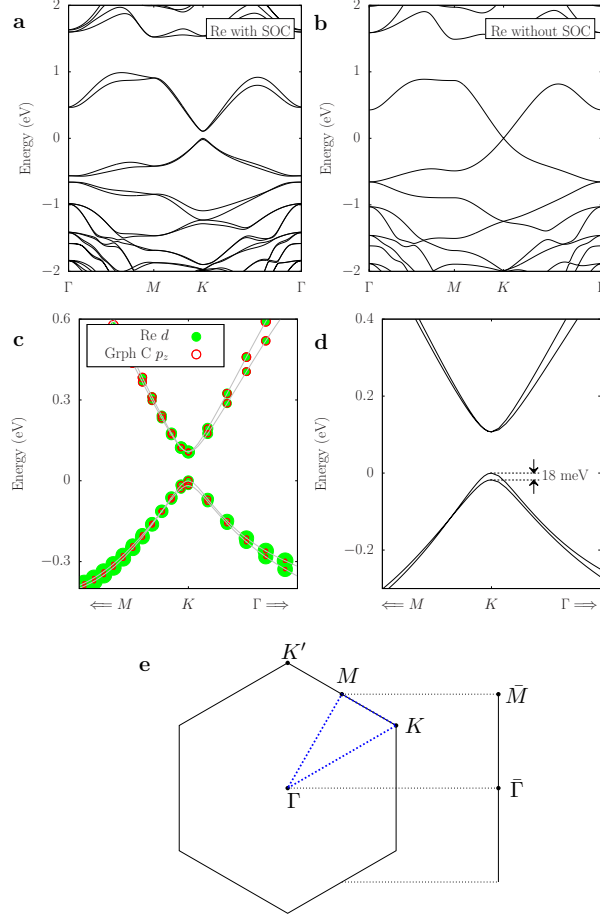


FIG. 2. Electronic band structure of Re-intercalated epitaxial graphene on SiC. The band structure (a) with and (b) without SOC. (c) Contributions from Re  $d$  and graphene C  $p_z$  states are denoted by green filled and red open circles, respectively. (d) The band structure near  $K$  with SOC. (e) The corresponding BZ.

can have any integer value (which physically corresponds to the number of edge states in the quantum Hall system), the topological number for the QSH classification is defined only up to mod 2 due to the presence of the time-reversal symmetry [27]. We find that the  $\mathbb{Z}_2$  invariant of the occupied bands in the Re-intercalated epitaxial graphene is nontrivial, i.e.,  $\nu = 1$ . Thus, the Re-intercalated graphene is a 2D topological insulator (or a QSH system).

Another notable effect of the SOC is spin degeneracy lift in the electronic band structure. In pristine graphene, the band structure is spin-degenerate at each  $k$ -point of the BZ due to the simultaneous presence of the spatial inversion symmetry and the time reversal symmetry as dictated by the relation  $E_{\vec{k}\uparrow} = E_{-\vec{k}\uparrow} = E_{\vec{k}\downarrow}$ , where the first and the second equality is given

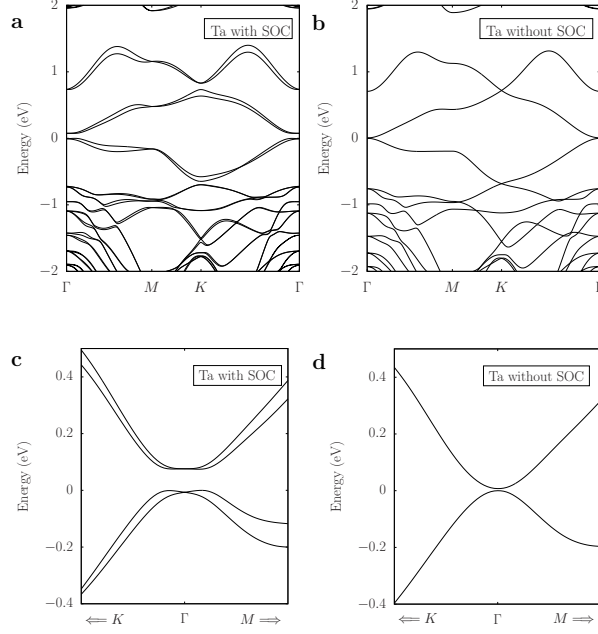


FIG. 3. Electronic band structure of Ta-intercalated epitaxial graphene. The band structure (a) with and (b) without SOC. The band structure near  $\Gamma$  (c) with and (d) without SOC.

by the inversion and the time-reversal symmetry, respectively. If the inversion symmetry is broken, the spin degeneracy will be lifted by the SOC in general. In the intercalated epitaxial graphene, the inversion symmetry is broken due to the presence of SiC substrate and the intercalation layer. Thus we have the spin splitting upon including the SOC. The size of the spin splitting in the valence band maximum (VBM) at  $K$  is calculated to be  $\approx 18$  meV (Fig. 2d). We note that a monolayer of the transition metal dichalcogenide  $\text{MoS}_2$  shares important common features with the intercalated graphene in that both systems have honeycomb-derived lattices, broken inversion symmetry, and sizable SOC strengths. We note that the monolayer  $\text{MoS}_2$  has a direct gap at  $K$  with larger VBM spin splitting of  $\approx 0.148$  meV [30].

The Ta-intercalated epitaxial graphene also shows a 2D topological insulator phase. The main difference in comparison with the Re intercalation is that the electronic band dispersion is quadratic (as opposed to linear) in the absence of the SOC (Fig. 3). Since Ta atom has 2 fewer electrons than Re, the Fermi energy shifts downward by two bands (including spin) compared with the Re intercalation, and the VBM and the conduction band minimum (CBM) lie near the  $\Gamma$  point of the BZ. The  $\mathbb{Z}_2$  invariant of the occupied bands is calculated to be 1, namely, the Ta-intercalated epitaxial graphene is also a 2D topological insulator

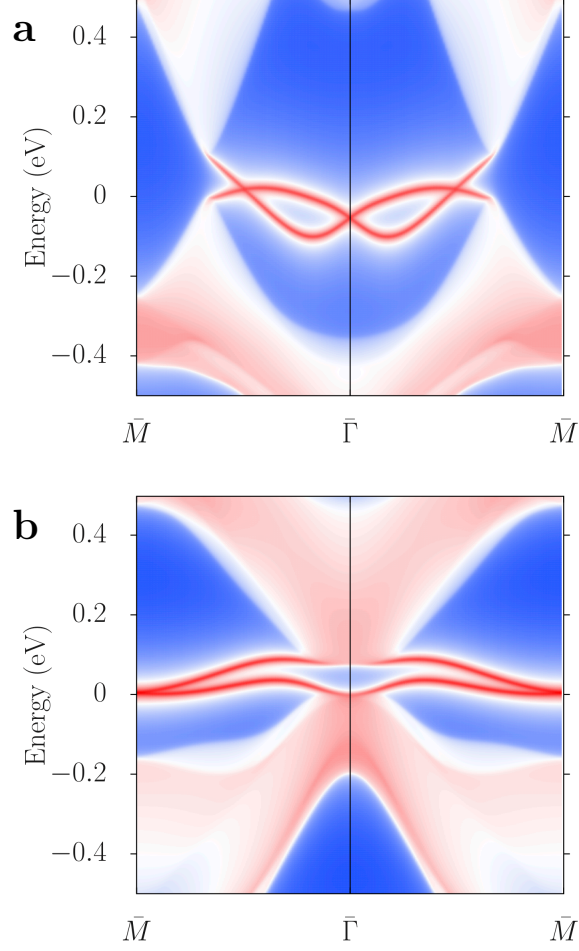


FIG. 4. Topological edge states in the intercalated epitaxial graphene. The edge state dispersion of (a) Re-intercalated and (b) Ta-intercalated epitaxial graphene.

(with a gap of  $\cong 74$  meV). Unlike the  $K$  point, the  $\Gamma$  point is a time-reversal invariant momentum satisfying  $-\vec{k} = \vec{k}$ , hence the spin degeneracy at  $\Gamma$  is protected by the time-reversal symmetry. Thus, the band dispersion near  $\Gamma$  shows the Rashba-type spin splitting (Fig. 3c) [31, 32]. The strength of the Rashba-type spin splitting can be represented by the Rashba parameter  $\alpha_R$  which is defined through the Bychkov-Rashba Hamiltonian

$$\mathcal{H}_R = \alpha_R(\hat{\gamma} \times \vec{k}) \cdot \vec{\sigma}, \quad (2)$$

where  $\hat{\gamma}$  and  $\vec{\sigma}$  denote the direction of the inversion symmetry breaking field (that is perpendicular to the graphene plane in our case) and Pauli matrices, respectively. According to our DFT band structure, the magnitude of the Rashba parameter  $\alpha_R$  in the valence band is estimated to be 0.21 eVÅ.

The existence of the topological boundary states is an important feature of a topological system. In general, topological boundary states are supposed to appear at a boundary between a topologically nontrivial system and a trivial one as far as the related symmetry (in our case the time-reversal symmetry) is not broken. The topological edge states are guaranteed to appear in the bulk energy gap in such a way that they cross the Fermi level at an odd number of points in half the BZ, connecting the bulk conduction and valence bands. They are robust conducting channel since the back-scattering is forbidden as far as the time-reversal symmetry is kept [14]. To calculate the dispersion of the boundary states, we construct Wannier functions from our DFT calculations and obtain the corresponding Hamiltonian. Then the edge state dispersion is calculated using the iterative Green's function method [24, 33–35] which gives energy- and momentum-resolved local density of states at the edge layers in the semi-infinite edge structure. The edge band structures are presented in Fig. 4. In both Re and Ta intercalation cases, we find that the edge states cross the Fermi energy (or any horizontal line in the bulk gap) at an odd number of crossing points along  $\bar{\Gamma}$ — $\bar{M}$ , as dictated by the bulk-boundary correspondence. This confirms that the bulk band topology is nontrivial in accordance with our  $\mathbb{Z}_2$  invariant calculations.

In conclusion, we showed that  $5d$  transition metal intercalation induces the topological band gap in the epitaxial graphene on the SiC substrate. It was found that the Re-intercalated graphene has linear Dirac cones with the sizable SOC-induced gap and the topological character of the occupied bands was verified by the nontrivial  $\mathbb{Z}_2$  invariant. In the Ta-intercalated graphene, we found the quadratic bands with the topological band gap. The broken inversion symmetry and the SOC induced the notable spin-splitting in both systems. Experimentally, the electronic band structures of the intercalated epitaxial graphene could be measured by ARPES [4–6, 25, 26], and the existence of the topological edge states could be validated via transport measurements [36]. Our results open a new avenue for the topological phase control of graphene and are potentially useful for spintronic applications of graphene and quantum computations.



## ACKNOWLEDGMENTS

This work was supported by the U.S. Department of Energy (DOE), Office of Science, Basic Energy Sciences, Materials Sciences and Engineering Division. The research was performed at Ames Laboratory, which is operated for the U.S. DOE by Iowa State University under Contract No. DE-AC02-07CH11358. Computations were performed through the support of the National Energy Research Scientific Computing Center, which is a DOE Office of Science User Facility operated under Contract No. DE-AC02-05CH11231.

- 
- [1] K. S. Novoselov, A. K. Geim, S. V. Morozov, D. Jiang, Y. Zhang, S. V. Dubonos, I. V. Grigorieva, and A. A. Firsov, *Science* **306**, 666 (2004).
  - [2] K. S. Novoselov, A. K. Geim, S. V. Morozov, D. Jiang, M. I. Katsnelson, I. V. Grigorieva, S. V. Dubonos, and A. A. Firsov, *Nature* **438**, 197 (2005).
  - [3] Y. Zhang, Y.-W. Tan, H. L. Stormer, and P. Kim, *Nature* **438**, 201 (2005).
  - [4] U. Starke, S. Forti, K. Emtsev, and C. Coletti, *MRS Bulletin* **37**, 11771186 (2012).
  - [5] I. Gierz, T. Suzuki, R. T. Weitz, D. S. Lee, B. Krauss, C. Riedl, U. Starke, H. Höchst, J. H. Smet, C. R. Ast, and K. Kern, *Phys. Rev. B* **81**, 235408 (2010).
  - [6] K. V. Emtsev, A. A. Zakharov, C. Coletti, S. Forti, and U. Starke, *Phys. Rev. B* **84**, 125423 (2011).
  - [7] B. M. Ludbrook, G. Levy, P. Nigge, M. Zonno, M. Schneider, D. J. Dvorak, C. N. Veenstra, S. Zhdanovich, D. Wong, P. Dosanjh, C. Straßer, A. Stöhr, S. Forti, C. R. Ast, U. Starke, and A. Damascelli, *Proceedings of the National Academy of Sciences* **112**, 11795 (2015), <https://www.pnas.org/content/112/38/11795.full.pdf>.
  - [8] S. Ichinokura, K. Sugawara, A. Takayama, T. Takahashi, and S. Hasegawa, *ACS Nano* **10**, 2761 (2016), pMID: 26815333.
  - [9] S. Schumacher, T. O. Wehling, P. Lazi, S. Runte, D. F. Frster, C. Busse, M. Petrovi, M. Kralj, S. Blgel, N. Atodiressei, V. Caciuc, and T. Michely, *Nano Letters* **13**, 5013 (2013).
  - [10] C. Riedl, C. Coletti, T. Iwasaki, A. A. Zakharov, and U. Starke, *Phys. Rev. Lett.* **103**, 246804 (2009).
  - [11] M. Kim, M. C. Tringides, M. T. Hershberger, S. Chen, M. Hupalo, P. A. Thiel, C.-Z. Wang,

- and K.-M. Ho, Carbon **123**, 93 (2017).
- [12] Y. Li, P. Chen, G. Zhou, J. Li, J. Wu, B.-L. Gu, S. B. Zhang, and W. Duan, Phys. Rev. Lett. **109**, 206802 (2012).
  - [13] M. Z. Hasan and C. L. Kane, Rev. Mod. Phys. **82**, 3045 (2010).
  - [14] X.-L. Qi and S.-C. Zhang, Rev. Mod. Phys. **83**, 1057 (2011).
  - [15] C. L. Kane and E. J. Mele, Phys. Rev. Lett. **95**, 226801 (2005).
  - [16] C. L. Kane and E. J. Mele, Phys. Rev. Lett. **95**, 146802 (2005).
  - [17] Y. Yao, F. Ye, X.-L. Qi, S.-C. Zhang, and Z. Fang, Phys. Rev. B **75**, 041401 (2007).
  - [18] G. Kresse and J. Hafner, Phys. Rev. B **47**, 558 (1993).
  - [19] G. Kresse and J. Furthmüller, Phys. Rev. B **54**, 11169 (1996).
  - [20] P. E. Blöchl, Phys. Rev. B **50**, 17953 (1994).
  - [21] G. Kresse and D. Joubert, Phys. Rev. B **59**, 1758 (1999).
  - [22] A. H. Gomes de Mesquita and IUCr, Acta Crystallographica **23**, 610 (1967).
  - [23] A. A. Mostofi, J. R. Yates, G. Pizzi, Y.-S. Lee, I. Souza, D. Vanderbilt, and N. Marzari, Computer Physics Communications **185**, 2309 (2014).
  - [24] Q. Wu, S. Zhang, H.-F. Song, M. Troyer, and A. A. Soluyanov, Computer Physics Communications **224**, 405 (2018).
  - [25] S. Watcharinyanon, L. I. Johansson, C. Xia, J. I. Flege, A. Meyer, J. Falta, and C. Virojanadara, Graphene **02**, 66 (2013).
  - [26] S. Watcharinyanon, L. I. Johansson, C. Xia, and C. Virojanadara, Journal of Applied Physics **111**, 083711 (2012).
  - [27] L. Fu and C. L. Kane, Phys. Rev. B **74**, 195312 (2006).
  - [28] T. Fukui and Y. Hatsugai, Journal of the Physical Society of Japan **76**, 053702 (2007).
  - [29] D. Xiao, Y. Yao, W. Feng, J. Wen, W. Zhu, X.-Q. Chen, G. M. Stocks, and Z. Zhang, Phys. Rev. Lett. **105**, 096404 (2010).
  - [30] Z. Y. Zhu, Y. C. Cheng, and U. Schwingenschlögl, Phys. Rev. B **84**, 153402 (2011).
  - [31] Y. A. Bychkov and E. I. Rashba, JETP Lett. **39**, 78 (1984).
  - [32] S. LaShell, B. A. McDougall, and E. Jensen, Phys. Rev. Lett. **77**, 3419 (1996).
  - [33] F. Guinea, C. Tejedor, F. Flores, and E. Louis, Phys. Rev. B **28**, 4397 (1983).
  - [34] M. P. L. Sancho, J. M. L. Sancho, and J. Rubio, Journal of Physics F: Metal Physics **14**, 1205 (1984).

- [35] M. P. L. Sancho, J. M. L. Sancho, J. M. L. Sancho, and J. Rubio, Journal of Physics F: Metal Physics **15**, 851 (1985).
- [36] M. König, S. Wiedmann, C. Brüne, A. Roth, H. Buhmann, L. W. Molenkamp, X.-L. Qi, and S.-C. Zhang, Science **318**, 766 (2007), <http://science.sciencemag.org/content/318/5851/766.full.pdf>.